

Electric Dipole Polarizability in ^{208}Pb as a Probe of the Symmetry Energy and Neutron Matter around $\rho_0/3$

Zhen Zhang¹ and Lie-Wen Chen^{*1,2}

¹*Department of Physics and Astronomy and Shanghai Key Laboratory for Particle Physics and Cosmology, Shanghai Jiao Tong University, Shanghai 200240, China*

²*Center of Theoretical Nuclear Physics, National Laboratory of Heavy Ion Accelerator, Lanzhou 730000, China*
(Dated: September 27, 2018)

It is currently a big challenge to accurately determine the symmetry energy $E_{\text{sym}}(\rho)$ and the pure neutron matter equation of state $E_{\text{PNM}}(\rho)$, even their values around saturation density ρ_0 . We find that the electric dipole polarizability α_{D} in ^{208}Pb can be determined uniquely by the magnitude of the $E_{\text{sym}}(\rho)$ or almost equivalently the $E_{\text{PNM}}(\rho)$ at subsaturation densities around $\rho_0/3$, shedding a light upon the genuine correlation between the α_{D} and the $E_{\text{sym}}(\rho)$. By analyzing the experimental data of the α_{D} in ^{208}Pb from RCNP using a number of non-relativistic and relativistic mean-field models, we obtain very stringent constraints on $E_{\text{sym}}(\rho)$ and $E_{\text{PNM}}(\rho)$ around $\rho_0/3$. The obtained constraints are found to be in good agreement with the results extracted in other analyses. In particular, our results provide for the first time the experimental constraints on $E_{\text{PNM}}(\rho)$ around $\rho_0/3$, which are in harmony with the recent determination of $E_{\text{PNM}}(\rho)$ from microscopic theoretical studies and potentially useful in constraining the largely uncertain many-nucleon interactions in microscopic calculations of neutron matter.

PACS numbers: 21.65.Ef, 21.65.Cd, 24.30.Cz, 21.30.Fe

1. Introduction.—The symmetry energy $E_{\text{sym}}(\rho)$ as well as the pure neutron matter equation of state (EOS) $E_{\text{PNM}}(\rho)$ plays key roles in the investigation of physical objects from microscopic neutron-rich nuclei to macroscopic neutron stars [1–4] and even in new physics beyond the standard model [5]. Although significant progress has been made in recent years in understanding the $E_{\text{sym}}(\rho)$ and $E_{\text{PNM}}(\rho)$ due to a lot of experimental, observational and theoretical efforts, accurate determination of $E_{\text{sym}}(\rho)$ and $E_{\text{PNM}}(\rho)$, even their values around saturation density $\rho_0 \approx 0.16 \text{ fm}^{-3}$, remains a big challenge (see, e.g., Refs. [6–11]). While heavy ion collisions and astrophysical observations provide two important approaches to constrain the symmetry energy from sub- to supra-saturation densities, nuclear structure probes usually can most effectively constrain the symmetry energy at subsaturation densities. It has been established that nuclear mass can put stringent constraint on the magnitude of $E_{\text{sym}}(\rho)$ around $2\rho_0/3$ [12–17] and the neutron skin thickness Δr_{np} of heavy nuclei can fix the density slope $L(\rho)$ of the symmetry energy around $2\rho_0/3$ [16–19]. At very low densities of $0.03\rho_0 < \rho < 0.2\rho_0$ and temperature in the range of $3 \sim 11 \text{ MeV}$ where the clustering effects are essential, the symmetry energy has been obtained using data from heavy ion collisions [20].

In contrast to the $E_{\text{sym}}(\rho)$, to our best knowledge, the only existing constraint on $E_{\text{PNM}}(\rho)$ is $E_{\text{PNM}}(\rho = 0.10 \text{ fm}^{-3}) = 11.4 \pm 1.0 \text{ MeV}$ obtained by analyzing the ground state properties of the doubly magic nuclei within the Skyrme-Hartree-Fock (SHF) approach [17]. Theoretically, microscopic studies based on chiral effective

field theory (ChEFT) [21, 22] and Quantum Monte Carlo (QMC) calculations [23–25] provide important information on $E_{\text{PNM}}(\rho)$. In these theoretical studies, the main uncertainty is due to the poorly known many-nucleon interactions. Therefore, experimental constraints on $E_{\text{PNM}}(\rho)$ are extremely useful to understand the largely uncertain many-nucleon interactions in microscopic calculations of neutron matter.

The nuclear electric dipole polarizability α_{D} [26] has been proposed to be a good probe of the symmetry energy [27]. However, their exact relationship has not yet been completely understood and even some controversial conclusions have been obtained in different analyses by examining the correlation between the α_{D} and the $E_{\text{sym}}(\rho)$ around ρ_0 [27–32]. In this work, we find that actually the α_{D} in ^{208}Pb can be determined uniquely by the magnitude of the $E_{\text{sym}}(\rho)$ or almost equivalently the $E_{\text{PNM}}(\rho)$ at much lower densities around $\rho_0/3$, shedding a light upon the genuine correlation between the α_{D} and the $E_{\text{sym}}(\rho)$. This finding together with the α_{D} in ^{208}Pb measured at the Research Center for Nuclear Physics (RCNP) [33] allows us to obtain quite precise constraints on $E_{\text{sym}}(\rho)$ and $E_{\text{PNM}}(\rho)$ around $\rho_0/3$. The present experimental constraints on $E_{\text{PNM}}(\rho)$ is potentially useful in constraining the poorly known many-nucleon interactions in the microscopic calculations of pure neutron matter.

2. The symmetry energy and α_{D} .—The EOS of asymmetric nuclear matter, defined by its nucleon specific binding energy, can be expanded as

$$E(\rho, \delta) = E_0(\rho) + E_{\text{sym}}(\rho)\delta^2 + O(\delta^4), \quad (1)$$

where $\rho = \rho_n + \rho_p$ is nucleon density and $\delta = (\rho_n - \rho_p)/(\rho_p + \rho_n)$ is the isospin asymmetry with ρ_n (ρ_p) denoting the neutron (proton) density; $E_0(\rho)$ represents the

*Corresponding author (email: lwchen@sjtu.edu.cn)

EOS of symmetric nuclear matter; $E_{\text{sym}}(\rho)$ is the symmetry energy and it can be expressed as

$$E_{\text{sym}}(\rho) = \frac{1}{2!} \frac{\partial^2 E(\rho, \delta)}{\partial \delta^2} \Big|_{\delta=0}. \quad (2)$$

The $E_0(\rho)$ is usually expanded around ρ_0 as $E_0(\rho) = E_0(\rho_0) + \frac{K_0}{2!} (\frac{\rho-\rho_0}{\rho_0})^2 + O((\frac{\rho-\rho_0}{\rho_0})^3)$ where the K_0 is the so-called incompressibility coefficient. The $E_{\text{sym}}(\rho)$ can also be expanded around a reference density ρ_r as $E_{\text{sym}}(\rho) = E_{\text{sym}}(\rho_r) + L(\rho_r)(\frac{\rho-\rho_r}{\rho_r}) + O((\frac{\rho-\rho_r}{\rho_r})^2)$ with $L(\rho_r) \equiv 3\rho_r \frac{dE_{\text{sym}}(\rho)}{d\rho} \Big|_{\rho=\rho_r}$ denoting the density slope of the symmetry energy at ρ_r . Neglecting the higher-order terms in Eq. (1) leads to the well-known empirical parabolic approximation $E_{\text{PNM}}(\rho) \approx E_0(\rho) + E_{\text{sym}}(\rho)$. It should be emphasized that in the present work, all the results for $E_{\text{sym}}(\rho)$ and $E_{\text{PNM}}(\rho)$ are obtained exactly in mean-field models without parabolic approximation.

The electric dipole polarizability α_D is proportional to the inverse energy-weighted sum of the electric dipole response [26] which is dominated by the isovector giant dipole resonance (IVGDR) — a nuclear collective oscillation of all the protons against all the neutrons with the symmetry energy $E_{\text{sym}}(\rho)$ acting as the restoring force [34]. Since the neutron and proton densities in the nuclear interior essentially do not change in the IVGDR, the α_D thus probes the symmetry energy not at ρ_0 but rather at much lower densities around the nuclear surface where matter with extreme isospin or even pure neutron (proton) matter may form in the oscillation.

A more quantitative preview about the α_D can be obtained from the macroscopic hydrodynamical model which predicts [35, 36]

$$\alpha_D = \frac{e^2}{24} \int \frac{r^2}{v_{\text{sym}}(\rho)} d^3r, \quad (3)$$

where r represents the radial coordinate in the nuclei and $v_{\text{sym}} = E_{\text{sym}}(\rho)/\rho$. Using an empirical 2-parameter Fermi distribution for the radial density distribution of nuclei and a simple parametrization of $E_{\text{sym}}(\rho) = 12.5(\rho/\rho_0)^{2/3} + 20(\rho/\rho_0)^\gamma$, one can find the α_D in Eq. (3) is dominated by the symmetry energy values at low densities around $\rho_0/3$. Moreover, using a leptodermous expansion in Eq. (3), Lipparini and Stringari [35] derived a simple expression of α_D as

$$\alpha_D = \frac{e^2}{12} \frac{A \langle r^2 \rangle}{b_v} \left(1 + \frac{5}{3} \frac{b_s}{b_v} A^{-1/3} \right), \quad (4)$$

where $\langle r^2 \rangle$ is the mean-square radius of the nucleus with mass number A , and b_v and b_s are the volume and surface symmetry coefficients which are related to the symmetry energy coefficient $a_{\text{sym}}(A)$ of finite nuclei with mass number A as [35]

$$a_{\text{sym}}(A) = \frac{1}{2} \frac{b_v}{1 + (b_s/b_v)A^{-1/3}}. \quad (5)$$

Using Eq. (4) and Eq. (5), Roca-Maza *et al.* [29] recently obtained a relation between the α_D and the symmetry energy parameters $E_{\text{sym}}(\rho_0)$ and $L(\rho_0)$ by invoking the simple relations $b_v = 2E_{\text{sym}}(\rho_0)$ and $b_s/b_v = \frac{9}{4} E_{\text{sym}}(\rho_0)/Q$ with Q being the surface stiffness coefficient [19, 37, 38]. On the other hand, substituting Eq. (5) into Eq. (4), one can then obtain a new and interesting relation

$$\alpha_D(A) = \frac{e^2}{24} \frac{A \langle r^2 \rangle}{a_{\text{sym}}(\frac{27}{125}A)}, \quad (6)$$

which suggests that the α_D of a nucleus with mass number A is inversely proportional to the symmetry energy coefficient of a nucleus with mass number $(\frac{3}{5})^3 A$ (e.g., for ^{208}Pb , $\alpha_D(A=208) \propto 1/a_{\text{sym}}(A=45)$). Considering the strong correlation between the $a_{\text{sym}}(A)$ and the $E_{\text{sym}}(\rho_A)$ at a specific density ρ_A [15, 19, 39, 40], one then expects that the α_D in ^{208}Pb should be strongly correlated with $E_{\text{sym}}(\rho)$ at $\rho = \rho_{A=45} \approx \rho_0/3$ [40].

The above discussions indicate that a model-independent linear correlation may exist between $1/\alpha_D$ in ^{208}Pb and the magnitude of the symmetry energy around $\rho_0/3$. As will be shown in the following, this genuine correlation can be exactly confirmed by the microscopic random-phase approximation (RPA) calculations based on non-relativistic and relativistic mean-field models. Then given $E_{\text{sym}}(\rho_0/3) \approx E_{\text{sym}}(\rho_0) - \frac{2}{9}L(\rho_0)$ or even better $E_{\text{sym}}(\rho_0/3) \approx E_{\text{sym}}(2\rho_0/3) - \frac{1}{6}L(2\rho_0/3)$, one can easily understand the dependence of α_D in ^{208}Pb on both $E_{\text{sym}}(\rho_0)$ and $L(\rho_0)$ [29] or on both $E_{\text{sym}}(2\rho_0/3)$ and $L(2\rho_0/3)$ [30]. This can also explain the relatively weak correlation of α_D in ^{208}Pb with the Δr_{np} [28] since the latter is essentially determined by $L(2\rho_0/3)$ [16].

3. *The symmetry energy from α_D in ^{208}Pb .*—In order to study the correlation of the α_D in ^{208}Pb with the symmetry energy value at different densities, we analyze the results from 62 representative non-relativistic and relativistic interactions which all give a good description of the ground state properties of finite nuclei but predict very different density dependence of the symmetry energy, including 47 Skyrme interactions [16, 41, 42] (i.e., BSk1, BSk2, BSk6, Es, Gs, KDE, KDE0v1, MSk7, MSL0, MSL1, NRAPR, Rs, SAMi, SGI, SGII, SK255, SK272, SKa, SkI3, SkM, SkMP, SkM*, SkP, SkS1, SkS2, SkS3, SkS4, SkSC15, SkT7, SkT8, SkT9, SKX, SKXce, SKXm, Skxs15, Skxs20, SLy4, SLy5, SLy10, v070, v075, v080, v090, v105, v110, Zs, Zs*) and 15 relativistic interactions involving FSU, NL3 and TF families [43, 44] together with DD-ME2 [45]. For the Skyrme interactions, we evaluate the α_D using the Skyrme-RPA program by Colò *et al.* [46] while for the relativistic interactions, we directly invoke the results of RPA calculations reported in Refs. [29, 44].

The obtained data-to-data relations between $10^3/\alpha_D$ in ^{208}Pb and the $E_{\text{sym}}(\rho_r)$ at $\rho_r = 0.02, 0.05, 0.08, 0.11$ and 0.16 fm^{-3} are displayed in Fig. 1. Also included in Fig. 1 are the linear fits together with the corresponding Pearson correlation coefficient r and the experimen-

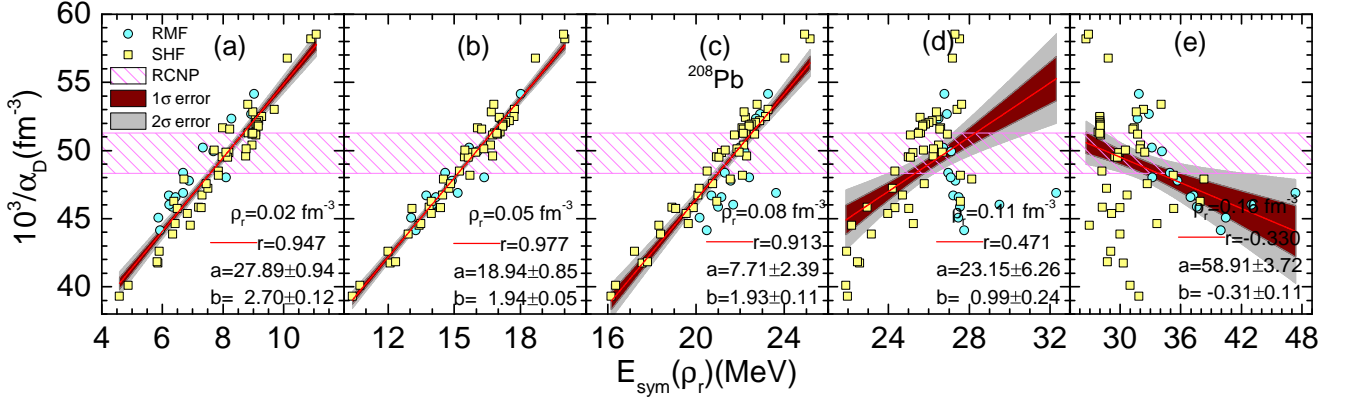


FIG. 1: $10^3/\alpha_D$ in ^{208}Pb vs. $E_{\text{sym}}(\rho_r)$ at $\rho_r = 0.02 \text{ fm}^{-3}$ (a), 0.05 fm^{-3} (b), 0.08 fm^{-3} (c), 0.11 fm^{-3} (d) and 0.16 fm^{-3} (e), predicted by a large number (62) of non-relativistic (SHF) and relativistic (RMF) models. The shaded regions correspond to linear fitting of $10^3/\alpha_D = a + bE_{\text{sym}}(\rho_r)$ with 1σ and 2σ confidence bands and r is the Pearson correlation coefficient. The red hatched band corresponds to the experimental result of $\alpha_D = 20.1 \pm 0.6 \text{ fm}^3$ from RCNP [33].

tal result of $\alpha_D = 20.1 \pm 0.6 \text{ fm}^3$ obtained from a high-resolution measurement at RCNP via polarized proton inelastic scattering at forward angles [33]. It is seen that the $1/\alpha_D$ exhibits a very strong linear correlation ($r = 0.977$) with the $E_{\text{sym}}(\rho)$ around $\rho_0/3$ (i.e., $\rho_r = 0.05 \text{ fm}^{-3}$), confirming the predictions of both hydrodynamical and droplet models discussed earlier. The correlation remains strong at densities below $\rho_0/3$ but it drops rapidly when the density is above about $\rho_0/2$.

For $\rho_r = 0.05 \text{ fm}^{-3}$, the linear fit gives

$$10^3/\alpha_D = (18.94 \pm 0.85) + (1.94 \pm 0.05)E_{\text{sym}}(\rho_r), \quad (7)$$

with α_D in fm^3 and $E_{\text{sym}}(\rho_r)$ in MeV. Substituting the experimental value of $\alpha_D = 20.1 \pm 0.6 \text{ fm}^3$ into Eq. (7)

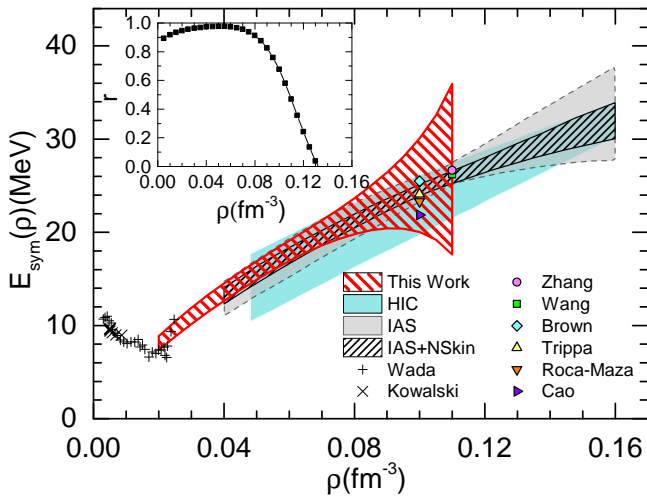


FIG. 2: Constraints on the symmetry energy $E_{\text{sym}}(\rho)$ as a function of density ρ (see text for the details). The inset shows the density dependence of the Pearson correlation coefficient r between $1/\alpha_D$ in ^{208}Pb and the $E_{\text{sym}}(\rho)$.

then leads to

$$E_{\text{sym}}(\rho_r) = 15.91 \pm (0.77)_{\text{exp}} \pm (0.63)_{\text{th}}, \quad (8)$$

where the uncertainties with “exp” and “th” are obtained from the propagation of the experimental uncertainty of α_D and the parameter errors in the linear fit which reflect the systematic errors, respectively. Consequently, one can obtain a stringent constraint of $E_{\text{sym}}(\rho_r = 0.05 \text{ fm}^{-3}) = 15.91 \pm 0.99 \text{ MeV}$. The similar analysis allows us to extract constraints on the symmetry energy value at other densities and the results from $\rho_r = 0.02 \text{ fm}^{-3}$ to 0.11 fm^{-3} are shown as red hatched band in Fig. 2. Shown in the inset in Fig. 2 is the density dependence of the r value. It should be emphasized that in the present work, the symmetry energy is obtained from the mean-field calculations without considering clustering effects. Indeed, at low densities ($\lesssim \rho_0/2$) uniform nucleonic matter may become unstable against cluster formation which may influence the symmetry energy. Theoretical studies [47] indicate that at zero temperature, only at very low densities (i.e., less than about 0.02 fm^{-3}) where the fraction of light clusters becomes significant, clustering effects are essential and increase significantly the symmetry energy. Therefore, the constraints on the symmetry energy at densities below 0.02 fm^{-3} are not shown in Fig. 2 although the r value is still large. At higher densities (e.g., above 0.11 fm^{-3}), effective constraints cannot be obtained as the r value becomes much smaller.

For comparison, we also shown in Fig. 2 the constraints from transport model analyses of mid-peripheral heavy ion collisions of Sn isotopes (HIC) [48] and the SHF analyses of isobaric analogue states (IAS) as well as combining additionally the neutron skin “data” (IAS+NSkin) in Ref. [15], and six constraints on the value of $E_{\text{sym}}(\rho)$ around $2/3\rho_0$ from binding energy difference between heavy isotope pairs (Zhang) [16], Fermi-energy difference in finite nuclei (Wang) [14], properties of doubly magic

nuclei (Brown) [17], the giant dipole resonance in ^{208}Pb (Trippa) [49], the giant quadrupole resonance in ^{208}Pb (Roca-Maza) [50] and the soft dipole excitation in ^{132}Sn (Cao) [51]. In addition, we also show the experimental results of the symmetry energies at densities below $0.2\rho_0$ and temperatures in the range $3 \sim 11$ MeV from the analysis of cluster formation in heavy ion collisions (Wada and Kowalski) [20]. It is remarkable to see that a single data of α_D in ^{208}Pb can give quite stringent constraints on $E_{\text{sym}}(\rho)$ around $\rho_0/3$ and the constraints are in very good agreement with other analyses. It is also interesting to see that the constrained $E_{\text{sym}}(\rho)$ around $\rho_0/7$ is nicely consistent with the results extracted from heavy ion collisions (Wada) which consider the clustering effects [20]. In addition, we note the $E_{\text{sym}}(\rho)$ has been predicted in microscopic calculations (see, e.g., Refs. [22, 52, 53]) and the results are consistent with the experimental constraints shown in Fig. 2.

4. *Neutron matter from α_D in ^{208}Pb .*—From the empirical parabolic approximation, one expects $E_{\text{PNM}}(\rho)$ should play a similar role as $E_{\text{sym}}(\rho)$ since $E_0(\rho)$ is relatively well determined, especially around $\rho_0/3$. Using the similar analysis as in Fig. 1, we indeed find a strong correlation between $1/\alpha_D$ in ^{208}Pb and $E_{\text{PNM}}(\rho)$ around $\rho_0/3$. Therefore, we can constrain $E_{\text{PNM}}(\rho)$ around $\rho_0/3$ in the similar way as constraining the $E_{\text{sym}}(\rho)$ and the results are shown as red hatched band in Fig. 3 in the density interval $0.015 \text{ fm}^{-3} < \rho < 0.11 \text{ fm}^{-3}$ with the corresponding density dependence of r shown in the inset. At lower densities (i.e., below 0.015 fm^{-3}), although the r value remains close to unit and the clustering effects are negligible in neutron matter, the constraints on $E_{\text{PNM}}(\rho)$ are not shown in Fig. 3 since the pairing effects, which are not considered in the mean-field calculations for $E_{\text{PNM}}(\rho)$, may become considerable [54]. We note the pairing effects on $E_{\text{PNM}}(\rho)$ are negligibly small for $\rho > 0.015 \text{ fm}^{-3}$ [54]. At higher densities (e.g., above 0.11 fm^{-3}), the r decreases rapidly and one cannot effectively constrain $E_{\text{PNM}}(\rho)$.

Also shown in Fig. 3 are the predictions from ChEFT using N^3LO potential in Ref. [21] (ChEFT) and in Ref. [22] (Wellenhofer), Auxiliary-Field Diffusion Monte Carlo (AFDMC) calculations employing local N^2LO ChEFT interaction with different cutoffs (QMC) [23], AFDMC calculations using adjusted nuclear force models by Gandolfi-Carlson-Reddy (GCR) [55], Auxiliary-Field QMC calculations with the N^3LO 2-body interactions plus the N^2LO 3-body interactions (Wlazłowski) [24], configuration interaction Monte Carlo calculations using nonlocal N^2LO chiral interaction (Roggero) [25], variational calculations by Akmal-Pandharipande-Ravenhall (APR) [52], the Bethe-Bruckner-Goldstone calculations using many-body expansion up to the three hole-line level of approximation with quark model interactions with the auxiliary potential of gap choice (GC) or continuous choice (BBG-QM 3h-gap and BBG-QM 3h-con) [56], and the self-consistent Green's function calculations that includes the effects of three-body forces

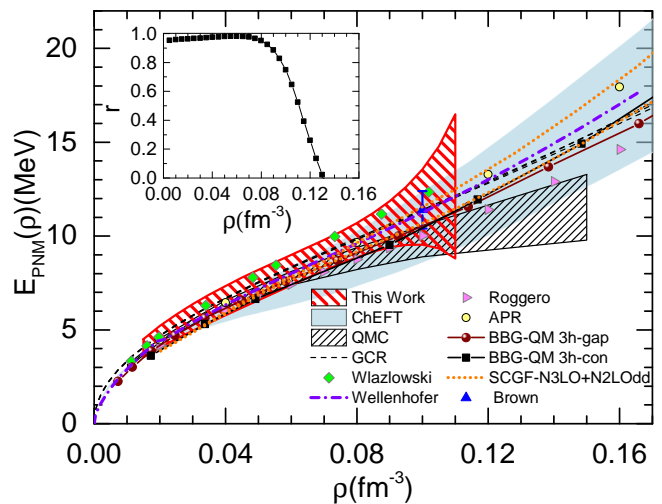


FIG. 3: Constraints and predictions for the pure neutron matter EOS $E_{\text{PNM}}(\rho)$ as a function of density ρ (see text for the details). The inset shows Pearson correlation coefficient r between $1/\alpha_D$ in ^{208}Pb and $E_{\text{PNM}}(\rho)$ as a function of ρ .

(SCGF-N3LO+N2LOdd) [57]. At $\rho = 0.1 \text{ fm}^{-3}$, the constraint $E_{\text{PNM}}(\rho = 0.10 \text{ fm}^{-3}) = 11.4 \pm 1.0 \text{ MeV}$ is also shown (Brown) [17].

One can see from Fig. 3 that our present analyses of the data on α_D in ^{208}Pb from RCNP give quite stringent constraints on $E_{\text{PNM}}(\rho)$ around $\rho_0/3$. To our best knowledge, our present results provide for the first time the experimental constraints on $E_{\text{PNM}}(\rho)$ around $\rho \approx \rho_0/3$. It is seen that our constraints are in excellent agreement with the predictions of APR, GCR and Wellenhofer as well as the constraint from Brown, and also consistent with other predictions. Interestingly, although our constraints are consistent with the predictions of both ChEFT and QMC within the uncertainty bands, there still exist some density regions where our constraints do not completely overlap with the uncertainty bands of ChEFT and QMC which are mainly due to the uncertainty of the many-body interactions. Therefore, our present experimental constraints on $E_{\text{PNM}}(\rho)$ are potentially useful for constraining the many-body interactions in ChEFT and QMC calculations, which may be significant to improve the prediction at higher densities.

5. *Conclusion.*—In summary, we have found that the electric dipole polarizability α_D in ^{208}Pb can be determined uniquely by the magnitude of the symmetry energy $E_{\text{sym}}(\rho)$ or almost equivalently the pure neutron matter EOS $E_{\text{PNM}}(\rho)$ at subsaturation densities around $\rho_0/3$, significantly deepening the understanding of the relation between the α_D and the $E_{\text{sym}}(\rho)$. This finding together with the α_D in ^{208}Pb measured at RCNP has allowed us to obtain very stringent constraints on $E_{\text{sym}}(\rho)$ and $E_{\text{PNM}}(\rho)$ around $\rho_0/3$. The present constraints should be less model dependent since they are based on a large set of both non-relativistic and relativistic models. Our results provide for the first time the

experimental constraints on $E_{\text{PNM}}(\rho)$ around $\rho_0/3$ which are potentially useful in constraining the many-nucleon interactions in microscopic calculations of neutron matter.

Acknowledgments.—We are grateful to Li-Gang Cao for helpful discussions on the Skyrme-RPA code. This work was supported in part by the National Basic Research Program of China (973 Program) under Contracts

No. 2015CB856904 and No. 2013CB834405, the NNSF of China under Grant Nos. 11275125 and 11135011, the “Shu Guang” project supported by Shanghai Municipal Education Commission and Shanghai Education Development Foundation, the Program for Professor of Special Appointment (Eastern Scholar) at Shanghai Institutions of Higher Learning, and the Science and Technology Commission of Shanghai Municipality (11DZ2260700).

-
- [1] J.M. Lattimer and M. Prakash, *Science* **304**, 536 (2004); *Phys. Rep.* **442**, 109 (2007).
- [2] A.W. Steiner, M. Prakash, J.M. Lattimer, and P. J. Ellis, *Phys. Rep.* **411**, 325 (2005).
- [3] V. Baran, M. Colonna, V. Greco, and M. Di Toro, *Phys. Rep.* **410**, 335 (2005).
- [4] B.A. Li, L.W. Chen, and C.M. Ko, *Phys. Rep.* **464**, 113 (2008).
- [5] C.J. Horowitz, S.J. Pollock, P.A. Souder, and R. Michaels, *Phys. Rev. C* **63**, 025501 (2001); T. Sil, M. Centelles, X. Viñas, and J. Piekarewicz, *Phys. Rev. C* **71**, 045502 (2005); D.H. Wen, B.A. Li, and L.W. Chen, *Phys. Rev. Lett.* **103**, 211102 (2009); H. Zheng, Z. Zhang, and L.W. Chen, *J. Cosmo. Astropart. Phys.* **08**, 011 (2014).
- [6] *Topical Issue Nuclear Symmetry Energy*, edited by B.-A. Li, A. Ramos, G. Verde, and I. Vidana, *Eur. Phys. J. A* **50**, (2014).
- [7] B.M. Tsang *et al.*, *Phys. Rev. C* **86**, 015803 (2012).
- [8] J.M. Lattimer, *Ann. Rev. Nucl. Part. Sci.* **62**, 485 (2012).
- [9] L.W. Chen, *Nuclear Structure in China 2012: Proceedings of the 14th National Conference on Nuclear Structure in China (NSC2012)* (World Scientific, Singapore, 2012), pp. 43-54 [arXiv:1212.0284].
- [10] B.A. Li *et al.*, *J. Phys.: Conf. Series* **413**, 012021 (2013) [arXiv:1212.1178].
- [11] C.J. Horowitz *et al.*, *J. Phys. G* **41**, 093001 (2014).
- [12] C.J. Horowitz and J. Piekarewicz, *Phys. Rev. Lett.* **86**, 5647 (2001).
- [13] R.J. Furnstahl, *Nucl. Phys.* **A706**, 85 (2002).
- [14] N. Wang, L. Ou, and M. Liu, *Phys. Rev. C* **87**, 034327 (2013).
- [15] P. Danielewicz and J. Lee, *Nucl. Phys.* **A922**, 1 (2014).
- [16] Z. Zhang and L.W. Chen, *Phys. Lett.* **B726**, 234 (2013).
- [17] B.A. Brown, *Phys. Rev. Lett.* **111**, 232502 (2013).
- [18] B.A. Brown, *Phys. Rev. Lett.* **85**, 5296 (2000).
- [19] M. Centelles, X. Roca-Maza, X. Viñas, and M. Warda, *Phys. Rev. Lett.* **102**, 122502 (2009); X. Roca-Maza, M. Centelles, X. Viñas, and M. Warda, *Phys. Rev. Lett.* **106**, 252501 (2011).
- [20] J.B. Natowitz *et al.*, *Phys. Rev. Lett.* **104**, 202501 (2010); S. Kowalski *et al.*, *Phys. Rev. C* **75**, 014601 (2007); R. Wada *et al.*, *Phys. Rev. C* **85**, 064618 (2012).
- [21] I. Tews, T. Krüger, K. Hebeler, and A. Schwenk, *Phys. Rev. Lett.* **110**, 032504 (2013).
- [22] C. Wellenhofer, J.W. Holt, and N. Kaiser, arXiv:1504.00177.
- [23] A. Gezerlis *et al.*, *Phys. Rev. Lett.* **111**, 032501 (2013).
- [24] G. Wlazłowski *et al.*, *Phys. Rev. Lett.* **113**, 182503 (2014).
- [25] A. Roggero, A. Mukherjee, and F. Pederiva, *Phys. Rev. Lett.* **112**, 221103 (2014).
- [26] O. Bohigas, N. Van Giai, and D. Vautherin, *Phys. Lett.* **B102**, 105 (1981).
- [27] P.-G. Reinhard and W. Nazarewicz, *Phys. Rev. C* **81**, 051303(R) (2010).
- [28] J. Piekarewicz *et al.*, *Phys. Rev. C* **85**, 041302(R) (2012).
- [29] X. Roca-Maza *et al.*, *Phys. Rev. C* **88**, 024316 (2013).
- [30] Z. Zhang and L.W. Chen, *Phys. Rev. C* **90**, 064317 (2014).
- [31] J. Piekarewicz, *Eur. Phys. J. A* **50**, 25 (2014).
- [32] G. Colò, U. Garg, and H. Sagawa, *Eur. Phys. J. A* **50**, 26 (2014).
- [33] A. Tamii *et al.*, *Phys. Rev. Lett.* **107**, 062502 (2011).
- [34] M. Goldhaber and E. Teller, *Phys. Rev.* **74**, 1046 (1948).
- [35] E. Lipparini and S. Stringari, *Phys. Lett.* **B112**, 421 (1982); *Phys. Rep.* **175**, 103 (1989).
- [36] J.M. Lattimer and A.W. Steiner, *Eur. Phys. J. A* **50**, 40 (2014).
- [37] W.D. Myers and W.J. Swiatecki, *Ann. Phys.* **84**, 186 (1974).
- [38] J. Meyer, P. Quentin, and B. Jennings, *Nucl. Phys.* **A385**, 269 (1982).
- [39] L.W. Chen, *Phys. Rev. C* **83**, 044308 (2011).
- [40] N. Alam, B.K. Agrawal, J.N. De, S.K. Samaddar, and G. Colò, *Phys. Rev. C* **90**, 054317 (2014).
- [41] M. Dutra *et al.*, *Phys. Rev. C* **85**, 035201 (2012).
- [42] X. Roca-Maza, G. Colò, and H. Sagawa, *Phys. Rev. C* **86**, 031306(R) (2012).
- [43] J. Piekarewicz, *Phys. Rev. C* **83**, 034319 (2011).
- [44] F.J. Fattoyev and J. Piekarewicz, *Phys. Rev. Lett.* **111**, 162501 (2013).
- [45] G. A. Lalazissis, T. Nikšić, D. Vretenar, and P. Ring, *Phys. Rev. C* **71**, 024312 (2005).
- [46] G. Colò, L.G. Cao, N. Van Giai, and L. Capelli, *Comput. Phys. Commun.* **184**, 142 (2013).
- [47] S. Typel, G. Ropke, T. Klahn, D. Blaschke, and H.H. Wolter, *Phys. Rev. C* **81**, 015803 (2010).
- [48] M.B. Tsang *et al.*, *Phys. Rev. Lett.* **102**, 122701 (2009).
- [49] L. Trippa, G. Colò, and E. Vigezzi, *Phys. Rev. C* **77**, 061304(R) (2008).
- [50] X. Roca-Maza *et al.*, *Phys. Rev. C* **87**, 034301 (2013).
- [51] L.G. Cao and Z.Y. Ma, *Chin. Phys. Lett.* **25**, 1625 (2008).
- [52] A. Akmal, V.R. Pandharipande, and D.G. Ravenhall, *Phys. Rev. C* **58**, 1804 (1998).
- [53] C. Drischler, V. Soma, and A. Schwenk, *Phys. Rev. C* **89**, 025806 (2014).
- [54] Z. Zhang and L.W. Chen, in preparation (2015).
- [55] S. Gandolfi, J. Carlson, and S. Reddy, *Phys. Rev. C* **85**, 032801(R) (2012).
- [56] M. Baldo and K. Fukukawa, *Phys. Rev. Lett.* **113**, 242501 (2014).
- [57] A. Carbone, A. Rios, and A. Polls, *Phys. Rev. C* **90**,

054322 (2014).